Single-molecule and single-nanoparticle SERS: from fundamental mechanisms to biomedical applications

X.-M. Qian and S. M. Nie*

Received 17th March 2008
First published as an Advance Article on the web 26th March 2008
DOI: 10.1039/b708839f

This *tutorial review* discusses a new class of colloidal metal nanoparticles that is able to enhance the efficiencies of surface-enhanced Raman scattering (SERS) by as much as 10^{14}–10^{15} fold. This enormous enhancement allows spectroscopic detection and identification of single molecules located on the nanoparticle surface or at the junction of two particles under ambient conditions. Considerable progress has been made in understanding the enhancement mechanisms, including definitive evidence for the single-molecule origin of fluctuating SERS signals. For applications, SERS nanoparticle tags have been developed based on the use of embedded reporter molecules and a silica or polymer encapsulation layer. The SERS nanoparticle tags are capable of providing detailed spectroscopic information and are much brighter than semiconductor quantum dots in the near-infrared spectral window. These properties have raised new opportunities for multiplexed molecular diagnosis and *in vivo* Raman spectroscopy and imaging.

Introduction

The observation of single-molecule surface-enhanced Raman scattering (SERS) has generated considerable interest both in the nanomaterials community and in the single-molecule spectroscopy community.[1–14] Following the initial work of Kneipp, Nie, and their co-workers,[1,2] independent research in several groups[3–10] has confirmed the enormously large enhancement factors on the order of 10^{14}–10^{15}. A novel finding is a class of optically "hot" nanoparticles that is unusually efficient for optical enhancement.[11–14] Furthermore, spatially isolated single particles and single aggregates have been shown to emit intense bursts of Stokes-shifted photons in an intermittent on–off fashion.[1,3–14] These results represent a dramatic example in which rare nanostructures with specific optical properties are selected from a large heterogeneous population for correlated spectroscopic and structural studies.

Based on previous SERS studies in bulk samples, it is believed that both a long-range electromagnetic (EM) effect and a short-range chemical effect are simultaneously operative. Schatz and co-workers[15] discussed the EM mechanism and its dependence on large-scale features (10–100 nm), while Otto[16] analyzed chemical enhancement and its dependence on atomic scale roughness. Moskovits and co-workers[17] developed a resonant fractal theory to explain surface Raman enhancement in extensively aggregated colloids. The EM mechanism arises from optical excitation of surface plasmon resonances in small metal particles, which leads to a significant increase in the electromagnetic field strength at the particle surface. In the chemical mechanism, molecules adsorbed at certain surface sites (such as atomic clusters, terraces, and steps) are believed to couple electronically with the surface,

Departments of Biomedical Engineering and Chemistry, Emory University and Georgia Institute of Technology, 101 Woodruff Circle, Suite 2001, Atlanta, GA 30322, USA. E-mail: snie@emory.edu; Fax: 404-727-3567; Tel: 404-712-8595

Dr Ximei Qian completed her PhD in physical chemistry under the guidance of Prof. C. Y. Ng, and received an Outstanding Dissertation Award from the University of California at Davis. In October 2003 she joined the molecular physics group with Prof. F. Merkt at ETH Zurich (Switzerland) as a postdoctoral fellow. Since January 2006, she has been working as a research associate with Prof. S. M. Nie at Emory University to develop Raman nanoparticle tags for in vivo *tumor targeting and spectroscopic detection.*

Dr Shuming Nie received his BS degree from Nankai University (China) in 1983, earned his MS and PhD degrees from Northwestern University (1984–1990), and did postdoctoral research at both Georgia Institute of Technology and Stanford University (1990–1994). He is currently the Wallace H. Coulter Distinguished Chair Professor in Biomedical Engineering at Emory University and the Georgia Institute of Technology, with joint appointments in chemistry, materials science and engineering, and hematology and oncology.

leading to an enhancement effect similar to resonance-Raman scattering.

At the single-particle level, recent theoretical work by Xu *et al.*[6–8] suggests that the maximum enhancement factor through electromagnetic fields is about 10^{11}. This enhancement is obtained only at the interstitial sites between two particles or at locations outside sharp surface protrusions. Experimental studies by Brus and co-workers[3–5] reveal that single-molecule SERS is not strongly correlated with surface plasmon resonance, and that the active sites are likely located at the junction between two Ag nanocrystals. This lack of direct correlation suggests that in addition to the EM component, there is a chemical or related mechanism that is not dependent on the electromagnetic field effect. In other words, surface plasmon excitation is necessary but not sufficient for observing single-molecule SERS. A further finding that cannot be explained by the EM mechanism alone is "blinking SERS," as briefly noted above.[1,3–14] This phenomenon is superficially similar to intermittent fluorescence emission that has been reported for single-quantum systems such as single fluorescent dye molecules and single semiconductor nanocrystals.[18–20] However, an important difference is that the SERS spectra show considerable fluctuations in both signal intensities and frequencies even under conditions where many molecules are expected to adsorb on a single particle or a single aggregate.[6–8] A hypothesis is that the "many-molecule" SERS spectra are still dominated by single molecules that are adsorbed at special surface sites or are located at a junction site between two particles. Here, we discuss recent progress in understanding the enhancement mechanism, the development of SERS nanoparticle tags, as well as recent work in using SERS nanotags for molecular, cellular, and *in vivo* imaging applications.

Fundamental mechanisms

Blinking and wandering

Single metal nanoparticles and nanoaggregates have been reported to emit intense bursts of surface-enhanced Raman scattering (SERS) in an intermittent on and off fashion (Fig. 1).[1,21] The characteristic "blinking" time scales range from milliseconds to seconds. Recent work indicates that blinking SERS contains both a thermo-activated component and a light-induced component.[21] Several lines of evidence suggest that the observed fluctuations are caused by thermally activated diffusion of individual molecules on the particle surface. Wavelength-resolved spectroscopy has further revealed that the fluctuating signals arise from surface-enhanced Raman scattering, and not from photoluminescence or elastic Rayleigh scattering (Fig. 2). The measured intensities represent the total Raman and background signals integrated over the spectral region of 557–663 nm (5–6 nm bandpass filter). Another important feature is that the SERS spectrum contains a significant background. This background is not due to residual R6G fluorescence but due to an emission continuum that is commonly observed in SERS.[22] The photon counts during the "off" periods are very low, indicating that the SERS signals and the background are correlated and fluctuate

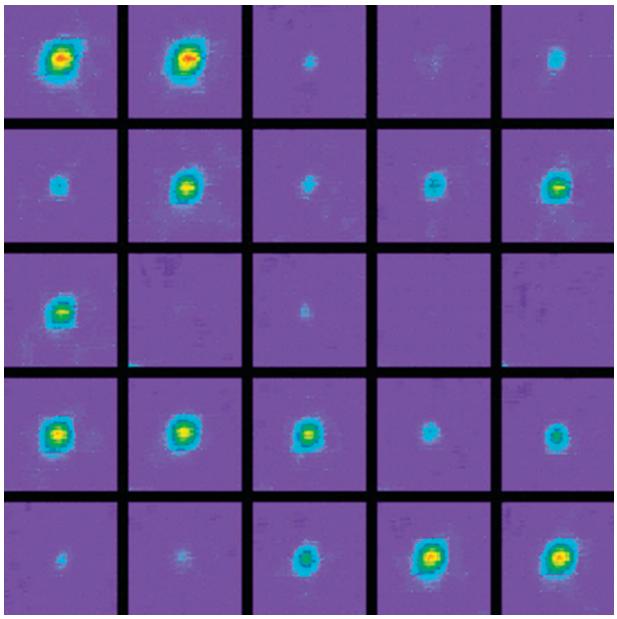

Fig. 1 Time-lapsed video images of intermittent light emission recorded from a single silver nanoparticle. The images are ordered from left-to-right with an elapsed time of 100 ms between images. The signal intensities are indicated by false colors. SERS video microscopy was accomplished using an inverted optical microscope, coupled with a 100× oil-immersion objective (N.A.1.3), a video-rate intensified CCD camera, and a high-speed frame grabber. Continuous-wave laser excitation at 514.5 nm was provided by an Ar^+ laser with a total excitation intensity (wide-field) of ~10 mW (130 W cm^{-2}). Adapted with permission from Emory *et al.* (ref. 21).

simultaneously (in phase). Brus and co-workers[3–5] reported a strong correlation of their SERS intensities and the background continuum with time. The photon bursts also appear to cluster with repeated bursts followed by dark periods. Statistical analysis of a large number of nanostructures indicates that the average on-time (t_{on}) is about 80 ms with 0.1-mW laser excitation (~0.5 μm focal spot) at room temperature. A further intriguing finding is spectral wandering; that is, the SERS signals suddenly change their frequencies. As first reported by Nie and Emory,[1] changes in the Raman signal frequencies of Rhodamine 6G are as large as 10 cm^{-1}. Even when sudden spectral changes are not observed, the Raman spectra obtained from different particles have slightly different vibrational frequencies.

Another source of spectral fluctuations is carbonaceous species[21] or other contamination from the photodecomposition of the adsorbates and dust. One needs to be extra careful when performing the experiments to differentiate the spurious SERS spectra of amorphous carbon from true single-molecule spectra.[23] It has been investigated that oxygen in ambient conditions plays an important role in causing SERS blinking. The blinking rate is more frequent and the intensity variations are more dramatic under ambient conditions than under inert conditions.[24] Other theory and experiments suggest that blinking is due to particle itself instead of adsorbate diffusion.[25] They have observed blinking under "adsorbate-free" conditions such as silver powder and vapor-deposited silver film itself.

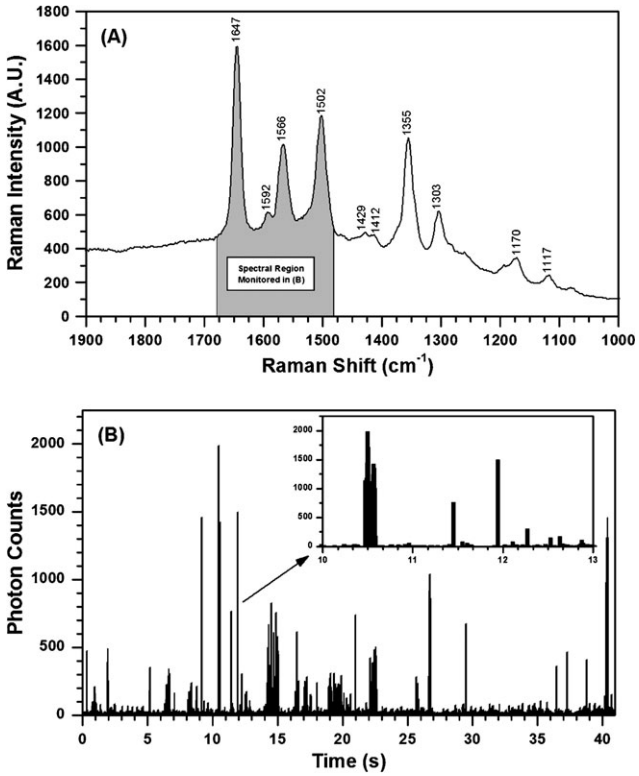

Fig. 2 Time-resolved studies of light emission from single Ag nanostructures. (a) SERS spectrum of R6G obtained with 514.5 nm excitation (1-μW confocal) and 10-s data integration. (b) Time-resolved SERS signals recorded with 0.1-mW laser power at 200 data points s^{-1}. A narrow bandpass filter was used to select the Raman lines at 1647, 1566 and 1502 cm^{-1} for measurement (shaded area). Adapted with permission from Nie and Emory (ref. 1).

SERS Active sites

A key question is the structure and properties of active sites on the particle surface. Previous studies suggest that these sites are likely adatoms, atomic clusters, sharp steps, or edges.[26,27] They are responsible for chemical enhancement *via* resonant charge-transfer and resonance-Raman-like enhancement.[28] In other words, strong electronic coupling between an adsorbed molecule and an active site generates new metal-to-ligand or ligand-to-metal charge transfer states that can be broadly excited at visible wavelengths. Previous work by Hildebrandt and Stockburger[29] suggests that the SERS-active sites are high-affinity binding sites (65 kJ per mole) associated with adsorbed anions such as Cl^- or Br^-.

To provide further insight into the nature of active sites, Doering and Nie[14] developed an integrated flow-injection and spectroscopy system to study the replacement of one adsorbed molecule by another. A key observation is that before halide treatment, the SERS spectrum often contains a broad background and weak signals from citrate (or its degradation products), but no detectable R6G signals. Upon halide addition, they found that the R6G spectrum suddenly replaces the citrate spectrum and appears over the background in a single step. The R6G signals then grow over a period of 10–30 min. This replacement behavior is consistent with the conclusion that the SERS spectrum is dominated by a single or a few molecules adsorbed at active sites. Furthermore, the results suggest that the active sites are initially empty or are occupied by citrate ions. The adsorption of halide ions facilitates the subsequent adsorption of R6G, but prevents the adsorption of citrate ions at the active sites.

In an elegant and decisive piece of work, Van Duyne and coworkers[30] used two isotopologues of Rhodamine 6G that offer unique vibrational signatures but with identical surface binding properties. When an average of one molecule is adsorbed per silver nanoparticle, only one isotopologue is typically observed in a dry nitrogen environment. The distribution of vibrational frequencies hidden under the ensemble average is revealed by examining the single-molecule spectra. At higher coverages and in humid environments, adsorbate interchanges occur due to competitive adsorption at a single site of the same location. Using 2D cross correlation, vibrational modes from different isotopologues are anti-correlated, indicating that the dynamic behavior is from multiple molecules competing for a single hot spot. This work has allowed hot-spot diffusion to be directly observed without analyzing the peak intensity fluctuations. It has accomplished a landmark task that many other groups were unable to do in the last 10 years.[11–14]

Chemical activation and deactivation

A major challenge in studying the mechanisms of SERS has been the difficulties in separating the chemical enhancement effect from the electromagnetic field effect. To address this question, Doering and Nie[14] directly examined chemical enhancement by using an integrated flow injection and ultrasensitive optical imaging/spectroscopy system. A key feature is that colloidal silver nanoparticles are immobilized on a glass surface inside a microflow device, and that single-particle SERS signals are observed in real time while the immobilized particles are treated by chemical reagents in the flow cell. *In situ* surface plasmon scattering studies of spatially isolated particles indicate that their electromagnetic properties do not change after chemical treatment. Thus, the observed SERS spectral changes should primarily come from chemical enhancement at surface active sites. Our experimental data reveal that three halide ions (Cl^-, Br^- and I^-) have a substantial activating effect, while other ions such as citrate, sulfate and fluoride have little or no effect on single-particle SERS. A "quenching" effect is observed for thiosulfate ions, which completely destroys the SERS activity. However, neither the halide ions nor thiosulfate produces detectable changes in surface plasmon scattering (both color and intensity) after 25 min of treatment (Fig. 3). As mentioned above, surface plasmon scattering provides an excellent measurement of the electromagnetic properties of single and aggregated colloidal nanoparticles. We believe that the observed activation/deactivation effect is primarily due to atomic-scale changes on the particle surface, not large-scale changes that would change the electromagnetic characteristics of the particles. Further wavelength-resolved studies of single-particle plasmon scattering could show small changes (5–10 nm) in the scattering spectra, but such small shifts are unlikely to cause significant changes in electromagnetic enhancement. In fact, previous studies have shown that the surface plasmon spectra are usually very

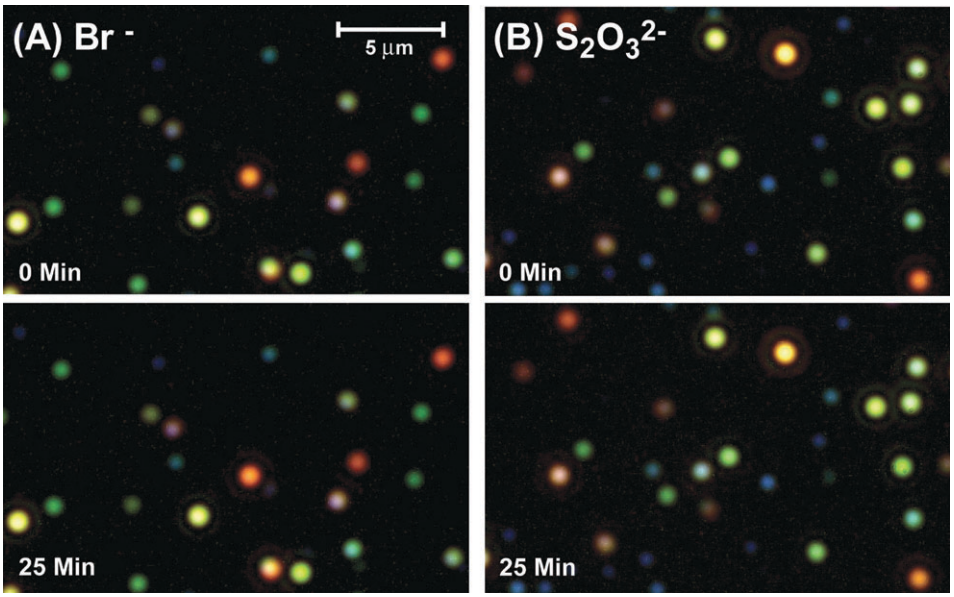

Fig. 3 Surface plasmon resonance scattering images of single immobilized nanoparticles before and after chemical treatment. Panel (A) shows particle scattering images before and after treatment with 10 mM bromide, while panel (B) shows particle scattering images before and after treatment with 10 mM thiosulfate. Note that no changes in scattering intensity or color were observed for any of the immobilized particles (either SERS active or inactive). Adapted with permission from Doering and Nie (ref. 14).

broad, and that single-molecule SERS is not directly correlated with surface plasmon scattering.[3–5]

Singles, dimers and aggregates

To compare SERS activity between single nanoparticles and small aggregates, Khan *et al.*[31] have examined whether optical SERS active sites are correlated with surface defects or particle junctions in high-resolution transmission electron microscopic (TEM) images. Their results do not show a strong correlation between high SERS activity and surface features. However, they do find that some immobilised single particles have similar averaged SERS intensities as that observed in dimers and trimers, but the signals are 3–4 times less than that of large aggregates. In terms of intensity fluctuations, single particles are found to give more reproducible SERS signals with a narrower range of on and off blinking times, in comparison with dimers and larger aggregates. This is understandable because molecules in the junction of two or more nanoparticles are strongly polarization-dependent. The orientation of these small aggregates may not align well with the incident laser beam, therefore the SERS signal intensity fluctuates dramatically due to the orthogonal selection rule. Although theory predicts that the electromagnetic field near the single nanoparticle surface is not as strong as that in a hot junction site, each particle can have a large number of adsorbed molecules. For ensemble colloidal systems, SERS intensities reach their maximal value at monolayer surface coverage. There are currently no consensuses on the percentage of single particles, dimers or aggregates that are optically ''hot''. This value is likely dependent on a number of factors such as particle size, reporter molecule adsorption, and surface activation.

It is true that SERS signals are enormously enhanced when a molecule is precisely localized at a hot junction spot between closely-coupled nanoparticles such as dimers or trimers with finite nano-gap geometries. In practice, however, it is very difficult to create such dimers or trimers with an analyte molecule sitting exactly at the junction. Also, metal nanoparticles are surrounded by Debye–Hückel ion clouds, which prevent other nanoparticles from contacting or close approaching by mutual electrostatic repulsion. This electrostatic barrier can be reduced with strong electrolytes, but this often induces uncontrolled particle aggregation and precipitation. One possible method for controlled aggregation is to add macromolecules or surfactants to provide steric hindrance, thereby preventing the direct contact of the diffusing nanoparticles.

Encapsulated SERS nanotags

The first generation of SERS tags was reported by Porter and co-workers[32] based on the co-adsorption of reporter molecules and targeting ligands onto metal nanoparticles. However, a major limitation of this approach is that the nanotags are prone to spectral changes and colloidal aggregation because they are not physically shielded from the external environments. To overcome this problem, several groups have employed various encapsulation strategies.[33–38] Polydivinylbenzene-coated SERS beads[33] are well-protected but require a secondary coating for bioconjugation and their micron-size is not ideal for molecular level detection in cells. Glass-coated tags are nanometer-sized and amenable to covalent bioconjugation. Fig. 4 illustrates the procedure of preparing silica-coated SERS nanotags and a TEM image with a gold core (dark black) and a silica shell (grey edge) to show the core–shell structure. The core–shell SERS nanotag contains three key components: a metallic core for optical enhancement, a reporter molecule for spectroscopic signature, and a

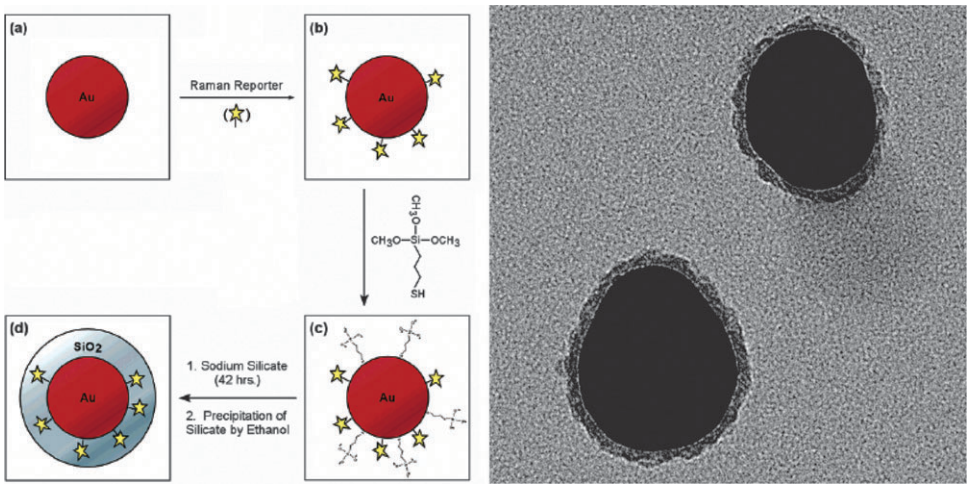

Fig. 4 Schematic illustration of the core–shell nanoparticle structure and the procedure for preparing silica-coated SERS-active gold colloids. (a) Colloidal gold particles in the size range of 55–65 nm, optimized for surface Raman enhancement at 632–647-nm excitation; (b) gold particles with an adsorbed Raman reporter; (c) gold particles with both the reporter and mercaptopropyltrimethoxysilane (a common coupling agent); and (d) silica-coated gold particles with a Raman spectroscopic reporter embedded at the core–shell boundary. Adapted with permission from Doering *et al*. (ref. 35).

silica shell for protection and conjugation.[35] This design has laid the foundation for practical bioanalytical applications utilizing the enormous enhancement effect, while avoiding interference from undesired analytes. Complete silica encapsulation ensures the stability of SERS nanotags in strong electrolyte conditions, but one limitation is that glass-coated particles tend to bind non-specifically to proteins and cell surfaces.[37] The silica encapsulation procedure also requires the reporter molecules to have multiple sulfur atom or isothiocyanate functional groups for stable surface adsorption.[35]

Our group has recently developed a new class of SERS tags that addresses the limitations encountered in previous studies.[38] The pegylated SERS tags consist of three elements: a ~60 nm citrate-stabilized gold particle, a Raman reporter molecule, and thiolated poly(ethylene glycol) (PEG-SH) (~5000 MW)—see Fig. 5. Measurements by UV-Vis absorption spectroscopy (Fig. 5(B)), transmission electron microscopy (TEM, Fig. 5(C)), and dynamic light scattering (DLS, Fig. 5(D)) reveal negligible aggregation upon addition of reporter dye—Malachite Green Isothiocyanate (MGITC) and PEG-SH to gold colloid. A small amount of MGITC addition does not alter the gold plasmon resonance peak at 535 nm, but a slight (~1 nm) red shift in absorbance is observed upon PEG-SH addition. The negatively stained TEM images show that the mean diameter of the Au core is ~57 nm and that the thickness of the PEG-SH coating is ~5 nm. Dynamic light scattering data indicate hydrodynamic size increases of ~2 nm and ~20 nm upon MGITC and PEG-SH addition, respectively. PEG-SH coating is an efficient and well-established method of protecting gold nanoparticles from aggregation in concentrated electrolyte solutions and organic solvents.[39,40] PEG-SH protected gold nanoparticles show minimal non-specific binding[41] and negligible cytotoxicity in intracellular delivery studies.[42] In addition, the use of heterobifunctional PEG provides a platform for efficient conjugation of biological targeting ligands.[43]

A surprising finding is that the PEG-SH coating process is compatible with non-sulfur containing reporter molecules bound to gold but stable enough to prevent free reporter molecules in the solution from accessing the gold surface. In contrast to silica encapsulation,[35] the PEG-SH coating does not displace adsorbed reporter molecules lacking multiple sulfur atom or isothiocyanate functional groups. Based on kinetic studies of alkanethiols of various chain lengths,[44] the PEG-SH (MW 5000) may have a much slower place-exchange reaction rate than the silica coupling agent (MW 179). A systematic study of reporter molecules such as Crystal Violet, Nile Blue, Basic Fuchsin and Cresyl Violet perchlorate reveals that all of these non-sulfur containing dyes are compatible with PEG-SH coating. In fact, SERS tags with crystal violet reporters are stable for more than 11 months. The dyes used in this study are all positively charged and contain extensively delocalized π-electron systems (3–4 phenyl rings), suggesting that a broad class of organic molecules can be used as sensitive Raman reporters for PEG-SH coated SERS tags.

Biomedical applications

There is considerable interest in SERS for ultrasensitive detection of biomolecules such as hemoglobin, glucose, cancer genes, pathogens, biological toxins and viruses during the last decade. SERS is a near-field probe which is sensitive to the local surrounding environment. Several groups published that SERS can be used as a pH nano-sensor for intracellular detection[45] and *ex vivo* environment[46] by functionalizing the surface of metal or core–shell nanoparticles with a pH sensitive SERS reporter molecule. Overall, there are two types of work related to SERS applications. In the first type, single-molecule SERS is used to examine the unique fingerprint spectra of pure analytes such as single DNA base pair and single hemoglobin molecules. Here the analyte molecule is believed to sit at a "hot spot" of a single particle or a nanoscale aggregate. In the second type of applications, SERS

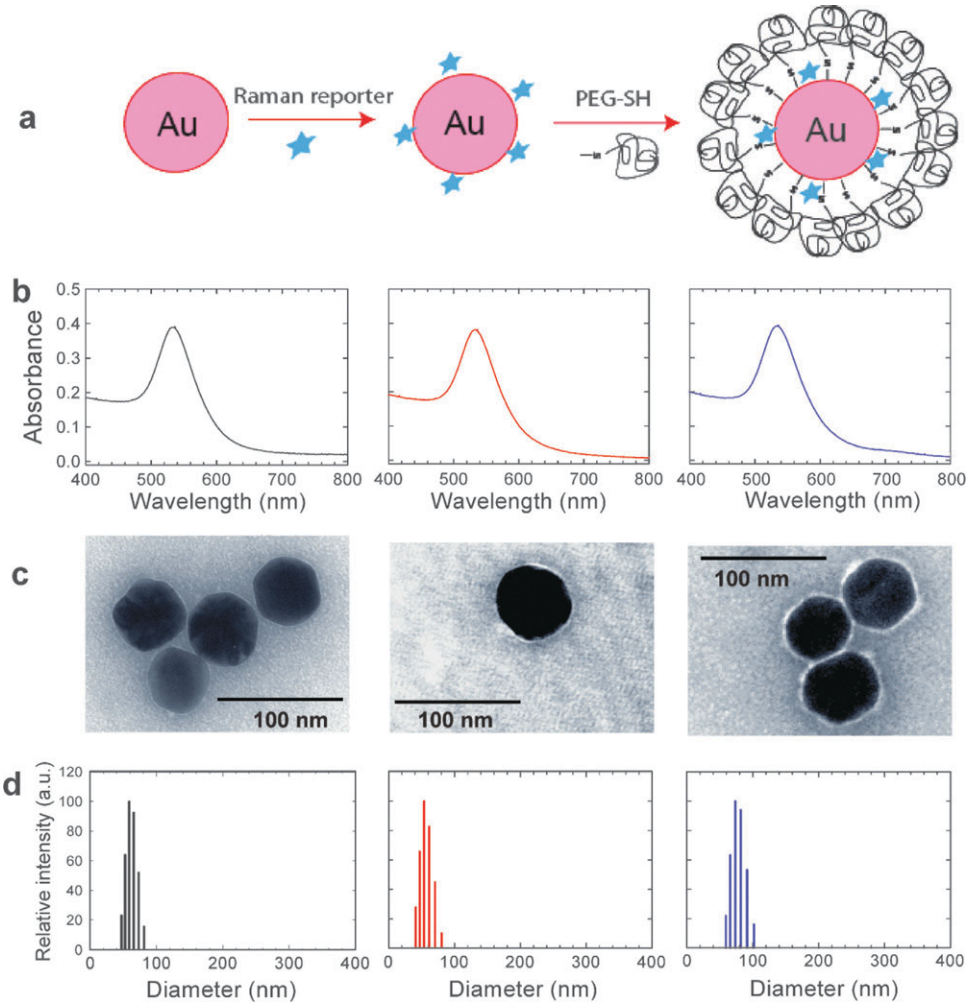

Fig. 5 Design and characterization of PEG-SH coated SERS nanotags. (A) Schematic illustration of tag assembly. Left panel: Au nanoparticles, Middle panel: Au–MGITC complex, Right panel: Au–MGITC-PEG-SH tag. (B) UV-Vis absorption spectra, (C) TEM images, and (D) DLS size distributions of each assembly state. Adapted with permission from Qian *et al.* (ref. 38).

spectra are obtained from an ensemble of nanoparticles covered by monolayer of molecules (100–100 000 depending on the particle size), yielding population-averaged data with well-defined frequencies and bandwidths. The spectral intensity and reproducibility can be well-controlled if the colloidal nanoparticle and the analytes are shielded locally from the environment. This design is much more robust for complex milieu such as cell culture medium or whole blood circulation where many heterogeneous analytes co-exist.

Biomarker detection

Recent work by Souza *et al.*[47] has achieved specific biomolecule targeting in a native cellular environment using SERS tags. Au–bacteriophage–imidazole complexes are used to label cells in solution, but the phage network has a high background SERS signal that limits the assay signal-to-noise ratio and does not protect the tags from spectral changes and aggregation. Huang *et al.*[48] demonstrated antibody-conjugated gold nanorods as potential cancer diagnostic markers using the surfactant CTAB as a reporter molecule for SERS readout. They coated gold nanorods with poly(styrene sulfonate) to stabilize the colloidal system and to reverse the surface charge from negative to positive. Hu *et al.*[49] linked Raman reporter with cyano groups in order to distinguish its vibrational peak from other contamination signals. Yu *et al.*[50] combined SERS Ag nanoshells with fluorescent dyes to examine the Raman signals from the reporter molecules together with fluorescent images in both cells and tissues.

Molecular profiling of single cells

Bioconjugated SERS nanotags have also been developed to recognize protein biomarkers on the surfaces of living cancer cells.[38] For cancer cell detection, targeted gold nanoparticles are prepared by using a mixture of thiol-PEG (~85%) and a heterofunctional PEG (SH-PEG-COOH) (~15%). The heterofunctional PEG is covalently conjugated to a single chain variable fragment antibody (ScFv, MW = 25 kD), a ligand that binds to the epidermal growth factor receptor (EGFR) with high specificity and affinity.[51] Human head and neck carcinoma cells (Tu686) are EGFR-positive (10^4–10^5 receptors per cell),[52] and are detected by strong SERS signals. In contrast, the human non-small cell lung carcinoma

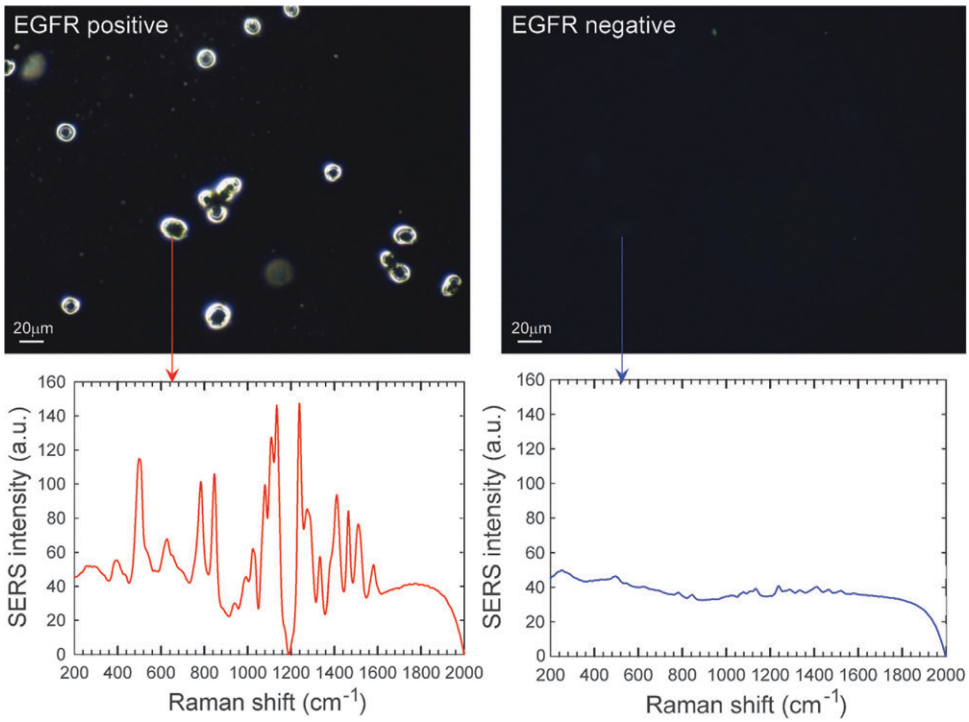

Fig. 6 SERS Spectra and correlated surface plasmon imaging of single cancer cells. Upper panels: Reflective mode dark-field images of live Tu686 cells (EGFR positive) and H520 cells (EGFR negative) tagged with ScFv-conjugated gold nanoparticles. The images were acquired with an Olympus Q-Color 5 CCD camera at an exposure time of 250 milliseconds. Lower panels: SERS spectra obtained from single cells as indicated by arrows. The Raman reporter dye is diethylthiatricarbocyanine (DTTC). Adapted with permission from Qian *et al.* (ref. 38).

(NCI-H520) do not express EGF receptors, showing little or no SERS signals. An infrared dye (diethylthiatricarbocyanine or DTTC) has been used as a spectroscopic reporter for surface-enhanced resonance-Raman scattering (SERRS) at 785 nm excitation. This resonance condition does not lead to photo-bleaching because the adsorbed dyes are protected from photo-degradation by efficient energy transfer to the metal particle. The resonance effect can further increase the surface-enhanced Raman signals by 10–100 fold, sensitive enough for Raman molecular profiling studies of single cancer cells (Fig. 6). This sensitivity is important for investigating the heterogeneous nature of cancer tissue specimens removed by surgery, and circulating tumor cells captured from peripheral blood samples. Single-cell profiling studies are of great clinical significance because EGFR is a validated protein target for monoclonal antibody and protein–kinase based therapies.[53,54]

In vivo tumor targeting and detection

To determine whether SERS spectra can be acquired from pegylated gold nanoparticles buried in animal tissues, Qian *et al.* injected small dosages of nanoparticles into subcutaneous and deep muscular sites in live animals.[38] The results demonstrate that highly resolved SERS signals are obtained from subcutaneous as well as deep muscular injections. The *in vivo* SERS spectra are identical to that obtained *in vitro* (saline solution), although the absolute intensities are attenuated by 1–2 orders of magnitude. Based on the high signal-to-noise ratios, it is estimated that the achievable penetration depth is about 1–2 cm for *in vivo* SERS tumor detection. For *in vivo* tumor targeting and spectroscopy, the gold nanoparticles conjugated with the ScFv antibody are injected systemically (*via* tail veins) into nude mice bearing a human head and neck tumor (Tu686). Fig. 7 shows SERS spectra obtained 5 h post nanoparticle injection by focusing a near-infrared (785 nm) laser beam to the tumor site or to other anatomical locations (*e.g.*, the liver or a leg). Significant differences are observed between the targeted and nontargeted nanoparticles in the tumor signal intensities, while the SERS signals from non-specific liver uptake are similar. This result indicates that the ScFv-conjugated gold nanoparticles are able to target EGFR-positive tumors *in vivo*. Time-dependent SERS data further indicate that nanoparticles are gradually accumulated in the tumor for 4–6 h, and that most of the accumulated particles stay in the tumor for more than 24–48 h.

All animal studies were based on protocols approved by the Institutional Animal Care and Use Committee of Emory University (Atlanta, Georgia, USA).

Concluding remarks

Colloidal gold SERS nanoparticles are dual-modality probes for optical and EM imaging, and could be used as a model system to design nanoparticles for molecular imaging and targeted therapy. A major task toward this goal is to develop "smart" nanoparticles that are able to avoid nonspecific organ uptake, and to target specific cells and organs *in vivo*. Since monodispersed gold colloids are available in a broad size range from 2 to 250 nm, nontoxic gold nanoparticles could be used to gain a better understanding of how particle size and surface coating affect their *in vivo* biodistribution and

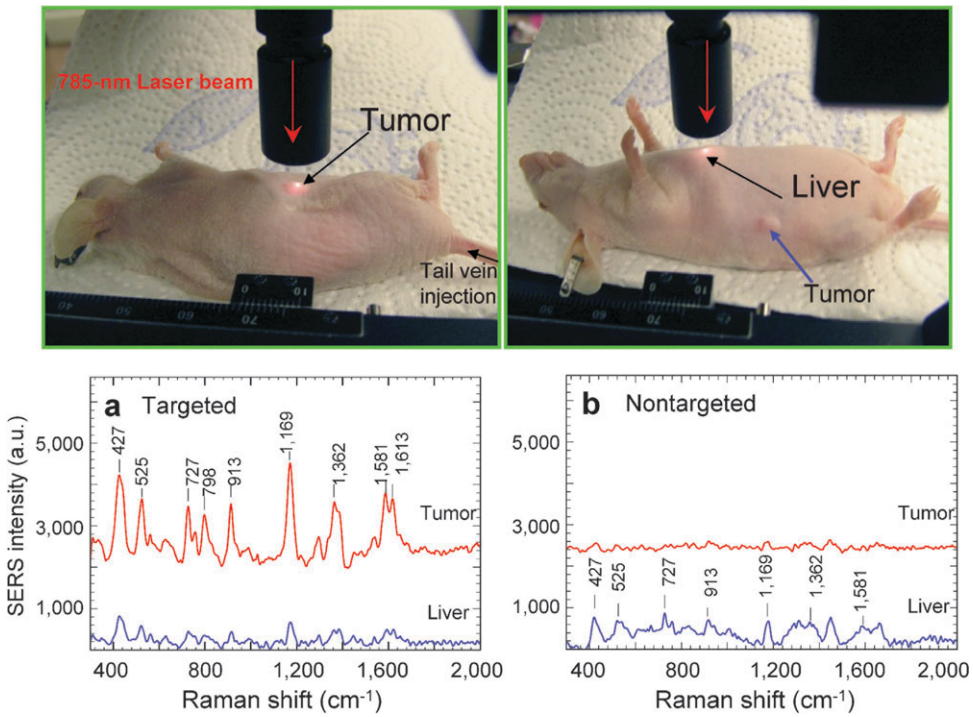

Fig. 7 *In vivo* cancer targeting and surface-enhanced Raman detection by using ScFv-antibody conjugated gold nanoparticles that recognize the tumor biomarker EGFR. Top: Photographs showing a laser beam focusing to the tumor site or to the anatomical location of liver. Lower: SERS spectra obtained from the tumor and the liver locations by using (a) targeted and (b) nontargeted nanoparticles. Two nude mice bearing human head and neck squamous cell carcinoma (Tu686) xenograft tumor (3 mm diameter) received 90 uL of ScFv EGFR-conjugated SERS tags or pegylated SERS tags (460 pM). The particles were administered *via* tail vein single injection. SERS spectra were taken 5 h post injection. *In vivo* SERS spectra were obtained from the tumor site (red) and the liver site (blue) with 2-s signal integration and at 785 nm excitation. The spectra were background subtracted and shifted for better visualization. The Raman reporter molecule is malachite green, with distinct spectral signatures as labeled. Laser power: 20 mW. Adapted with permission from Qian *et al.* (ref. 38).

targeting. Furthermore, therapeutic drugs can be conjugated to gold nanoparticles by covalent or noncovalent methods, allowing the development of integrated diagnostic and therapeutic nanoparticle agents.

Acknowledgements

This work was supported by grants from the US Air Force Office of Research and the National Cancer Institute (R01CA108468, U54CA119338, and P50CA128613).

References

1 S. M. Nie and S. R. Emory, *Science*, 1997, **275**, 1102–1106.
2 K. Kneipp, Y. Wang, H. Kneipp, L. T. Perelman, I. Itzkan, R. Dasari and M. S. Feld, *Phys. Rev. Lett.*, 1997, **78**, 1667–1670.
3 A. M. Michaels, M. Nirmal and L. E. Brus, *J. Am. Chem. Soc.*, 1999, **121**, 9932–9939.
4 A. M. Michaels, J. Jiang and L. Brus, *J. Phys. Chem. B*, 2000, **104**, 11965–11971.
5 K. A. Bosnick, J. Jiang and L. E. Brus, *J. Phys. Chem. B*, 2002, **106**, 8096–8099.
6 H. X. Xu, E. J. Bjerneld, M. Kall and L. Borjesson, *Phys. Rev. Lett.*, 1999, **83**, 4357–4360.
7 E. J. Bjerneld, P. Johansson and M. Kall, *Single Mol.*, 2000, **1**, 239–248.
8 H. X. Xu, J. Aizpurua, M. Kall and P. Apell, *Phys. Rev. E*, 2000, **62**, 4318–4324.
9 P. J. Moyer, J. Schmidt, L. M. Eng and A. J. Meixner, *J. Am. Chem. Soc.*, 2000, **122**, 5409–5410.
10 T. L. Haslett, L. Tay and M. Moskovits, *J. Chem. Phys.*, 2000, **113**, 1641–1646.
11 S. R. Emory, W. E. Haskins and S. M. Nie, *J. Am. Chem. Soc.*, 1998, **120**, 8009–8010.
12 S. R. Emory and S. Nie, *J. Phys. Chem. B*, 1998, **102**, 493–497.
13 J. T. Krug, G. D. Wang, S. R. Emory and S. M. Nie, *J. Am. Chem. Soc.*, 1999, **121**, 9208–9214.
14 W. E. Doering and S. M. Nie, *J. Phys. Chem. B*, 2002, **106**, 311–317.
15 K. L. Kelly, E. Coronado, L. L. Zhao and G. C. Schatz, *J. Phys. Chem. B*, 2003, **107**, 668–677.
16 A. Otto, *J. Raman Spectrosc.*, 2002, **33**, 593–598.
17 D. P. Tsai, J. Kovacs, Z. H. Wang, M. Moskovits, V. M. Shalaev, J. S. Suh and R. Botet, *Phys. Rev. Lett.*, 1994, **72**, 4149–4152.
18 R. M. Dickson, A. B. Cubitt, R. Y. Tsien and W. E. Moerner, *Nature*, 1997, **388**, 355–358.
19 W. P. Ambrose, P. M. Goodwin, J. C. Martin and R. A. Keller, *Science*, 1994, **265**, 364–367.
20 M. Nirmal, B. O. Dabbousi, M. G. Bawendi, J. J. Macklin, J. K. Trautman, T. D. Harris and L. E. Brus, *Nature*, 1996, **383**, 802–804.
21 S. R. Emory, R. A. Jensen, T. Wenda, M. Y. Han and S. M. Nie, *Faraday Discuss.*, 2006, **132**, 249–259.
22 M. Moskovits, *Rev. Mod. Phys.*, 1985, **57**, 783–826.
23 K. F. Domke and B. Pettinger, *Phys. Rev. B*, 2007, **75**, 236401.
24 A. Kudelski, *J. Phys. Chem. B*, 2006, **110**, 12610–12615.
25 P. C. Andersen, M. L. Jacobson and K. L. Rowlen, *J. Phys. Chem. B*, 2004, **108**, 2148–2153.
26 J. R. Lombardi, R. L. Birke, T. H. Lu and J. Xu, *J. Chem. Phys.*, 1986, **84**, 4174–4180.
27 P. Kambhampati, C. M. Child and A. Campion, *J. Chem. Soc., Faraday Trans.*, 1996, **92**, 4775–4780.
28 A. Otto, A. Bruckbauer and Y. X. Chen, *J. Mol. Struct.*, 2003, **661**, 501–514.

29 P. Hildebrandt and M. Stockburger, *J. Phys. Chem.*, 1984, **88**, 5935–5944.
30 J. A. Dieringer, R. B. Lettan II, K. A. Scheidt and R. P. Van Duyne, *J. Am. Chem. Soc.*, 2007, **129**, 16249–16256.
31 I. Khan, D. Cunningham, R. E. Littleford, D. Graham, W. E. Smith and D. W. McComb, *Anal. Chem.*, 2006, **78**, 224–230.
32 J. Ni, R. J. Lipert, G. B. Dawson and M. D. Porter, *Anal. Chem.*, 1999, **71**, 4903–4908.
33 A. F. McCabe, C. Eliasson, R. A. Prasath, A. Hernandez-Santana, L. Stevenson, I. Apple, P. A. G. Cormack, D. Graham, W. E. Smith, P. Corish, S. J. Lipscomb, E. R. Holland and P. D. Prince, *Faraday Discuss.*, 2006, **132**, 303–308.
34 L. Sun, C. X. Yu and J. Irudayaraj, *Anal. Chem.*, 2007, **79**, 3981–3988.
35 W. E. Doering and S. M. Nie, *Anal. Chem.*, 2003, **75**, 6171–6176.
36 S. P. Mulvaney, M. D. Musick, C. D. Keating and M. J. Natan, *Langmuir*, 2003, **19**, 4784–4790.
37 S. Kaufmann and M. Tanaka, *ChemPhysChem*, 2003, **4**, 699–704.
38 X.-M. Qian, X. H. Peng, D. O. Ansari, Q. Yin-Goen, G. Z. Chen, D. M. Shin, L. Yang, A. N. Young, M. D. Wang and S. M. Nie, *Nat. Biotechnol.*, 2008, **26**, 83–90.
39 W. P. Wuelfing, S. M. Gross, D. T. Miles and R. W. Murray, *J. Am. Chem. Soc.*, 1998, **120**, 12696–12697.
40 M. C. Daniel and D. Astruc, *Chem. Rev.*, 2004, **104**, 293–346.
41 S. F. Yu, S. B. Lee, M. Kang and C. R. Martin, *Nano Lett.*, 2001, **1**, 495–498.
42 D. Shenoy, W. Fu, J. Li, C. Crasto, G. Jones, C. Dimarzio, S. Sridhar and M. Amiji, *Int. J. Nanomed.*, 2006, **1**, 51–58.
43 L. R. Hirsch, J. B. Jackson, A. Lee, N. J. Halas and J. West, *Anal. Chem.*, 2003, **75**, 2377–2381.
44 A. C. Templeton, M. P. Wuelfing and R. W. Murray, *Acc. Chem. Res.*, 2000, **33**, 27–36.
45 J. Kneipp, H. Kneipp, B. Wittig and K. Kneipp, *Nano Lett.*, 2007, **7**, 2819–2823.
46 S. W. Bishnoi, C. J. Rozell, C. S. Levin, M. K. Gheith, B. R. Johnson, D. H. Johnson and N. J. Halas, *Nano Lett.*, 2006, **6**, 1687–1692.
47 G. R. Souza, D. R. Christianson, F. I. Staquicini, M. G. Ozawa, E.Y. Snyder, R. L. Sidman, J. H. Miller, W. Arap and R. Pasqualini, *Proc. Natl. Acad. Sci. USA*, 2006, **103**, 1215–1220.
48 X. H. Huang, I. H. El-Sayed, W. Qian and M. A. El-Sayed, *Nano Lett.*, 2007, **7**, 1591–1597.
49 Q. Y. Hu, L. L. Tay, M. Noestheden and J. P. Pezacki, *J. Am. Chem. Soc.*, 2007, **129**, 14–15.
50 K. N. Yu, S. M. Lee, J. Y. Han, H. Park, M. A. Woo, M. S. Noh, S. K. Hwang, J. T. Kwon, H. Jin, Y. K. Kim, P. J. Hergenrother, D. H. Jeong, Y. S. Lee and M. H. Cho, *Bioconjugate Chem.*, 2007, **18**, 1155–1162.
51 R. S. Herbst and D. M. Shin, *Cancer*, 2002, **94**, 1593–1611.
52 C. W. M. Reuter, M. A. Morgan and A. Eckardt, *Br. J. Cancer*, 2007, **96**, 408–416.
53 J. G. Paez, P. A. Janne, J. C. Lee, S. Tracy, H. Greulich, S. Gabriel, P. Herman, F. J. Kaye, N. Lindeman, T. J. Boggon, K. Naoki, H. Sasaki, Y. Fujii, M. J. Eck, W. R. Sellers, B. E. Johnson and M. Meyerson, *Science*, 2004, **304**, 1497–1500.
54 T. J. Lynch, D. W. Bell, R. Sordella, S. Gurubhagavatula, R. A. Okimoto, B. W. Brannigan, P. L. Harris, S. M. Haserlat, J. G. Supko, F. G. Haluska, D. N. Louis, D. C. Christiani, J. Settleman and D. A. Haber, *New Engl. J. Med.*, 2004, **350**, 2129–2139.

